Coassembly of Synthetic Segments of Shaker K^+ Channel within Phospholipid Membranes[†]

Hadas Peled-Zehavi,[‡] Isaiah T. Arkin,[§] Donald M. Engelman,[§] and Yechiel Shai*,[‡]

Department of Membrane Research and Biophysics, Weizmann Institute of Science, Rehovot, 76100 Israel, and Department of Molecular Biophysics & Biochemistry, Yale University School of Medicine, New Haven, Connecticut 06510

Received December 18, 1995; Revised Manuscript Received March 27, 1996[⊗]

ABSTRACT: Increasing evidence suggests that membrane-embedded hydrophobic segments can interact within the phospholipid milieu of the membrane with varying degrees of specificity and thus contribute to the folding and oligomerization of proteins. We have used synthetic peptides corresponding to segments from the hydrophobic core of the Shaker potassium channel as a model system to study interactions between membrane-embedded segments. Three synthetic segments of the Shaker K^+ channel, comprising the hydrophobic S2, S3, and S4 sequences, were used, and their secondary structure, their interactions with, and orientation within phospholipid membranes were examined. Secondary structure studies revealed that though S3 and S4 both adopt certain fractions of α-helical structures in membrane mimetic environments, the α-helical content of S3 is lower. Both S3 and S4 bind strongly to zwitterionic phospholipids, with partition coefficients in the order of 10^4 and 10^5 M^{-1}. ATR-FTIR studies showed that while the S4 peptide is oriented parallel to the membrane surface, S3 tends to a more transmembranal orientation. Enzymatic cleavage experiments demonstrated that the presence of S3 induces some change in the proteolytic accessibility of the S4 segment. Resonance energy transfer measurements, done in high lipid/peptide molar ratios, revealed that S3 and S4 cannot self-associate in zwitterionic phospholipid vesicles but can associate with each other and with the S2 segment of the channel. Furthermore, S3 does not interact with the homologous S4 region from the first repeat of the eel sodium channel, demonstrating specificity in the interactions. These results are in line with data indicating that functionally important interactions indeed exist between the negatively charged S2 and S3 regions and the positively charged S4 region [Papazian, D. M., et al. (1995) *Neuron 14*, 1293−1301; Planells-Cases, R., et al. (1995) *Proc. Natl. Acad. Sci. U.S.A. 92*, 9422−9426]. From a broader point of view, these results provide further support to the notion that interactions (either specific or nonspecific) may exist between transmembrane segments of integral membrane proteins and therefore can contribute to their assembly and organization.

Interactions between membrane-embedded segments of integral proteins are receiving a growing amount of attention. Such interactions are likely to contribute to the folding and oligomerization of integral proteins and can vary in their degree of specificity [see review by Lemmon and Engelman (1994)]. Ion channels are abundant integral membrane proteins that allow the passage of specific ions through the phospholipid membrane barrier, an essential step in many cellular processes (Hille, 1992). The voltage-activated K^+ channels, which are a large and diverse group within the family of voltage-activated ion conducting channels, are divided into several subfamilies. They are assumed to be formed by the coassembly of four polypeptide monomers of about 70 Kd each (Catterall, 1988; MacKinnon, 1991; Liman et al., 1992). Sequence analysis of these K^+ channel monomers suggests that each of them consists of six hydrophobic segments (S1−S6), each long enough to form a transmembrane helix, and an S5−S6 linker (the H5 region) proposed to form part of the lumen of the channel. They also include long N- and C-terminal domains. Although heteromultimeric functional channels might be formed by the assembly of monomers from different members of the same subfamily of K^+ channels, combinations of monomers from different subfamilies do not yield functional channels (Covarrubias et al., 1991; Christie et al., 1990; Isacoff et al., 1990; McCormack et al., 1990; Ruppersberg et al., 1990). Yet, it is not clear which structural components are involved in the folding of the monomers, in their assembly to form functional channels, or in the specific recognition needed for this "discriminative" assembly process. Subunit interactions within the hydrophobic core region were indicated in the assembly process, as well as sites in the intracellular N-terminal domains of the channels, which seem to be crucial to the process of "discriminative" assembly (Li et al., 1992; Shen et al., 1993; Babila et al., 1994; Lee et al., 1994). Furthermore, interactions between segments and subunits of the channel have functional importance in the assembled channel as well, as was shown for the H5 segments (Kirsch et al., 1993; Taglialatela et al., 1994) and the S4 segments (Papazian et al., 1995). Thus, the voltage-gated potassium channels present an interesting and relevant system to examine interactions between membrane-embedded segments.

[†] This research was supported in part by grants from the Joseph Cohn Center for Biomembrane Research and the Pearl Levine Foundation for Research in the Neurosciences at the Weizmann Institute of Science to Y.S. and by grants from The National Science Foundation and The National Foundation For Cancer Research to D.M.E.

* To whom correspondence should be addressed, at the Department of Membrane Research and Biophysics, Weizmann Institute of Science, Rehovot, 76100, Israel. Phone: 972-8-9342711. Fax: 972-8-9344112.

[‡] Weizmann Institute of Science.

[§] Yale University School of Medicine.

[⊗] Abstract published in *Advance ACS Abstracts,* May 1, 1996.

S0006-2960(95)02988-6 CCC: $12.00 © 1996 American Chemical Society

The S4 segment is highly conserved in the Shaker-like potassium channels and also exists in each of the four domains of sodium and calcium channel α-subunits. S4 has a basic residue at every third or fourth position. Because of this unique structure, it was proposed that the S4 may be the voltage sensor of the channel. In accordance with this model, it was shown that replacement of each of the basic residues in the S4 segment with neutral or a different basic residue produces changes in the voltage-dependent properties of the channel (Papazian et al., 1991). The effects of the different mutations vary, demonstrating that structural features other than electrostatic interactions between the electric field and the basic residues play a part in voltage gating. Indeed, the existence of functionally important short-range hydrophobic interactions between the S4 segment and its immediate surroundings was demonstrated using conservative mutations of hydrophobic residues within the S4 sequence (Lopez et al., 1991). Cooperative interactions between individual subunits were also suggested in the gating of the channel (Tytgat & Hess, 1992). It was proposed (Greenblatt et al., 1985; Montal, 1990) and recently shown (Koopmann et al., 1995; Ledwell et al., 1995; Papazian et al., 1995; Planelles-Cases et al., 1995) that S4 alone cannot account for the voltage dependence of the channel, and that acidic residues in the S2 and S3 segments might also be involved in the voltage sensing of the channel. These acidic residues might form electrostatic interactions with positive charges on the S4 segment (Bezanilla et al., 1995; Papazian et al., 1995; Planelles-Cases et al., 1995).

The aim of this study was to examine the S2, S3, and S4 segments of the Shaker potassium channel, and their mutual interactions, using a spectroscopical approach. Thus, chemically synthesized peptides comprising the S4 segment (amino acids 358−383) and the N-terminal extended S3 segment (amino acids 304−332) of the Shaker potassium channel were synthesized and fluorescently labeled. Previously synthesized S2 segment (Peled & Shai, 1994) and S4 segment from the first repeat of the eel sodium channel (Rapaport et al., 1992) were also utilized. It was found that S3 and S4 are at least partially α-helical in hydrophobic environment, and that each interacts strongly with phospholipid membranes. ATR-FTIR[1] studies showed that while the S4 peptide is oriented parallel to the membrane surface, S3 tends to a more transmembranal orientation. The ability of the peptides to self-associate and to associate with each other and with the S2 segment was assessed by RET studies. The results demonstrate that although neither S3 nor S4 is able to self-associate, they can associate with the S2 segment and with each other. These results support recent evidence that interactions indeed exist between the negatively charged S2 and S3 regions and the positively charged S4 region (Papazian et al., 1995; Planelles-Cases et al., 1995). Furthermore, some specificity is evident in those interactions. Though the S3 segment associate with the S4 segment of the Shaker potassium channel, it does not associate with the S4 segment from the sodium channel, demonstrating specificity in the interactions. From a broader point of view, these results provide further support to the notion that interactions exist between transmembrane segments of integral membrane proteins and therefore can contribute to the assembly and organization of integral membrane proteins as well as their function [see review by Lemmon and Engelman (1994)].

[1] Abbreviations: BOC, butyloxycarbonyl; CD, circular dichroism; DCC, dicyclohexylcarbodiimide DIEA, diisopropylethylamine; DMF, dimethyl formamide; DMPC, L-α-dimyristoylphosphatidylcholine; ATR-FTIR, attenuated total reflection Fourier transform infrared; HEPES, *N*-(2-hydroxyethyl)piperazine-*N*′-2-ethanesulfonic acid; HOBT, 1-hydroxybenzotriazole; NBD, 7-nitrobenz-2-oxa-1,3-diazole-4-yl; Pam, (phenylacetamido)methyl; PC, egg phosphatidylcholine; Rho, 5(and 6)-tetramethylrhodamine; RP-HPLC, reverse-phase high-performance liquid chromatography; SDS, sodium dodecyl sulfate; SUV, small unilamellar vesicles; TFA, trifluoroacetic acid; TFE, trifluoroethanol.

MATERIALS AND METHODS

Materials. BOC-amino acid-PAM [(Phenylacetamido)-methyl] resins were purchased from Applied Biosystems (Foster City, CA), and BOC amino acids were obtained from Peninsula Laboratories (Belmont, CA). Other reagents for peptide synthesis included trifluoroacetic acid (TFA) (Sigma), *N*,*N*-diisopropylethylamine (DIEA) (Aldrich, distilled over ninhydrin), dicyclohexylcarbodiimide (DCC) (Fluka), 1-hydroxybenzotriazole (HOBT) (Pierce), methylene chloride, and dimethyl formamide (DMF) (Bio-lab). Egg phosphatidylcholine (PC) was purchased from Lipid Products (South Nutfield U.K.), and L-α-dimyristoylphosphatidylcholine (DMPC) was purchased from Avanti Polar Lipids (Alabaster, AL). Octyl β-glucoside was purchased from Sigma (St. Louis, MO). Cholesterol (extra pure) was supplied by Merck (Darmstadt, Germany) and recrystallized twice from ethanol. 5-(and-6)-Carboxytetramethylrhodamine succinimidyl ester was obtained from Molecular Probes (Eugene, OR). NBD (4-fluoro-7-nitrobenz-2-oxa-1,3-diazole) was obtained from Sigma. Sodium dodecyl sulfate (SDS) was purchased from BDH (England). All other reagents were of analytical grade. Buffers were prepared using double glass-distilled water.

Peptide Synthesis and Fluorescent Labeling. The peptides were synthesized by the solid phase method on amino acid-PAM resins (0.075 mequiv) (Merrifield et al., 1982). At the end of the synthesis, the resin-bound peptides were cleaved from the resins by HF and extracted with ether after HF evaporation. S2 and S3 were dissolved in TFE [2:1 (w/v) solution] and were purified on an analytical CN reverse-phase DuPont column or analytical C4 reverse-phase Vydac column (300 Å pore size), respectively. S4 was dissolved in 50% acetonitrile/water [2:1 (w/v) solution], and purified on a analytical C18 reverse-phase Vydac column (300 Å pore size). The columns were eluted in 40 min, at a flow rate of 0.6 mL/min, using a linear gradient of acetonitrile in water in the presence of 0.1% TFA (v/v). A linear gradient of 25−80% acetonitrile in water was used for S4, a gradient of 30−90% was used for S2, and a gradient of 35−90% was used for S3. The peptides were subjected to amino acid analysis in order to confirm their composition.

Labeling of the N-termini of the peptides with fluorescent probes was achieved by labeling the resin-bound peptides as previously described (Rapaport & Shai, 1991, 1992). Resin-bound peptides (30−40 mg, 10−25 μmol) were treated with TFA [50% (v/v) in methylene chloride] to remove the BOC protecting group from the N-terminal amino group of the attached peptides. The resin-bound peptides were then reacted with either (i) 5-(and-6)-carboxytetramethylrhodamine succinimidyl ester (3−4 equiv) in dry DMF containing 2.5% (v/v) DIEA or (ii) 4-fluoro-7-nitrobenz-2-oxa-1,3-diazole in dry DMF. These two reactions led to the formation of resin-bound N^1-Rho-peptides or N^1-NBD-peptides, respectively. After 96 h, the mixtures were washed thoroughly with DMF

and methylene chloride. The peptides were then cleaved from the resins by HF and purified by reverse-phase HPLC as described above.

Preparation of Small Unilamellar Vesicles. Small unilamellar vesicles (SUV) were prepared by sonication of egg PC as previously described (Shai et al., 1990). Briefly, dry lipid and cholesterol (10:1 w/w) were dissolved in a $CHCl_3$/MeOH mixture (2:1 v/v). The solvents were then evaporated under a stream of nitrogen, and the lipids (at a concentration of 7.2 mg/mL) were put under vacuum for 1 h and then resuspended in the appropriate buffer, via vortex mixing. The resultant lipid dispersion was then sonicated for 5−10 min in a bath-type sonicator (J. P. SELECTA, s.a.) until clear. The lipid concentration of the supernatant was determined by phosphorus analysis (Bartlett et al., 1959). Vesicles were visualized using a JEOL JEM 100B electron microscope (Japan Electron Optics Laboratory Co. Tokyo, Japan). Vesicles prepared in this fashion are unilamellar, with an average diameter of 20−50 nm (Papahadjopoulos & Miller, 1967).

CD Spectroscopy. CD spectra were measured at room temperature using a Jasco J-500A spectropolarimeter after calibrating the instrument with (+)-10-camphorsulfonic acid. Cylindrical fused quartz optical cells of 0.5 or 2 mm path length were used. Spectra were obtained at wavelengths of 195−250 nm. Six to eight scans were taken at a scan rate of 20 nm/min. The peptides were scanned either in 40% TFE or in 35 mM SDS in buffer (16.7 mM NaCl, 4.2 mM HEPES-SO_4^{2-}, pH 7.3). The peptides were scanned at concentrations of 0.7×10^{-5} to 2.3×10^{-5} M as estimated by quantitative amino acid analysis. Fractional helicities (Greenfield & Fasman, 1969; Wu et al., 1981) were calculated as follows:

$$f_h = \frac{([\theta]_{222} - [\theta]^0_{222})}{[\theta]^{100}_{222}}$$

where $[\theta]_{222}$ is the experimentally observed mean residue ellipticity at 222 nm, and values for $[\theta]^0_{222}$ and $[\theta]^{100}_{222}$, corresponding to 0% and 100% helix content at 222 nm, are estimated at 2000 and 30 000 deg·cm^2/dmol, respectively (Chen et al., 1974; Wu et al., 1981).

Infrared Spectroscopy. The samples were prepared by dissolving lyophilized peptides in a solution of 10% octyl β-glucoside to a final concentration of 1 mg/mL. An equal amount of solution containing 20 mg/mL DMPC and 5% octyl β-glucoside was added to the protein, and reconstitution of the peptides into the phospholipids was achieved by exhaustive dialysis into a buffer containing 0.1 mM $NaPO_4$, pH 6.8. FTIR spectra were recorded on a Nicolet Magna 550 spectrometer purged with N_2 and equipped with a MCT/A detector. One thousand interferograms recorded at a spectral resolution of 4 cm^{-1} were averaged for each sample. Interferograms were processed using 1.0 filling and Happ-Genzel apodization. For polarized ATR-FTIR spectra the spectrometer was equipped with a KRS-5 wire grid polarizer (0.25 μm spacing, Grasbey Specac, Kent, U.K.). The sample (∼400 μL) was dried on the surface of a Ge internal reflection element (52 × 20 × 2 mm) and placed in a variable angle ATR accessory (Grasbey Specac, Kent, U.K.).

Analysis of Orientation from ATR-FTIR Dichroism. The electric field amplitudes of the evanescent wave are given by Harrick (1967):

$$E_x = 2(\sin^2 \Phi - {n_{21}}^2)^{1/2} \cos \Phi/[(1 - {n_{21}}^2)^{1/2}[(1 + {n_{21}}^2) \sin^2 \Phi - {n_{21}}^2]^{1/2}]$$

$$E_y = 2 \cos \Phi/(1 - {n_{21}}^2)^{1/2}$$

$$E_z = 2 \sin \Phi \cos \Phi/[(1 - {n_{21}}^2)^{1/2}[(1 + {n_{21}}^2) \sin^2 \Phi - {n_{21}}^2)^{1/2}]$$

where Φ is the angle of incidence between the IR beam and the internal reflection element (45°), and n_{21} is the ratio between the refractive indices of the sample ($n_2 = 1.43$) and the internal reflection element ($n_1 = 4.0$) (Wolfe & Zissis, 1978; Fringeli et al., 1989; Tamm & Tatulian, 1993). These equations are based on the assumption that the thickness of the deposited film (> 20 μm) is much larger than the penetration depth (∼1 μm) of the evanescent wave [see Harrick (1967)]. The electric field components together with the dichroic ratio [defined as the ratio between absorption of parallel ($A_\parallel$) and perpendicular ($A_\perp$) polarized light, $R^{ATR} \equiv A_\parallel/A_\perp$] are used to calculate an order parameter defined as

$$S \equiv 3/2\langle \cos^2 \theta \rangle - 1/2$$

with the following equation:

$$S = 2({E_x}^2 - R^{ATR}{E_y}^2 + {E_z}^2)/[(3 \cos^2 \alpha - 1)({E_x}^2 - R^{ATR}{E_y}^2 - 2{E_z}^2)]$$

where θ is the angle between the helix director and the normal of the internal reflection element, and α is the angle between the helix director and the transition dipole moment of the amide I vibrational mode (39°, Tsuboi, 1962). Order parameters of 1.0 and −0.5 correspond to helical orientations parallel and perpendicular to the membrane normal, respectively. Lipid order parameters are obtained from the lipid methylene symmetric (2852 cm^{-1}) and asymmetric (2924 cm^{-1}) stretching modes using the same equation by setting $\alpha = 90°$.

NBD Fluorescence Measurements. Changes in the fluorescence of NBD-labeled peptides were measured upon binding to PC vesicles. A small volume of concentrated solution of NBD-labeled peptides dissolved in DMSO was added to 400 μL of buffer (50 mM Na_2SO_4, 25 mM HEPES-SO_4^{2-}, pH 6.8) containing 240−300 μM PC, SUV (1:1 w/w) to get final concentration of 0.1−0.2 μM NBD-labeled peptide. Thus, a lipid/peptide molar ratio in which most of the peptide is bound to lipid was established. Emission spectra were measured at room temperature, using a Perkin-Elmer LS-50B Spectrofluorometer with the excitation set at 467 nm, using a 5 nm slit.

Binding Experiments. Binding experiments were done as described before (Rapaport & Shai, 1991). Briefly, PC SUV were added successively to 0.1−0.2 μM of NBD-labeled S4 or S3 at room temperature. Alternatively, a fixed amount of NBD-labeled peptide (0.1−0.2 μM) was added to separate cuvettes containing increasing amounts of vesicles. Fluorescence intensities were measured as a function of the lipid/peptide molar ratio on a Perkin-Elmer LS-50B spectrofluorometer, with the excitation set at 467 nm, using a 10 nm slit, and the emission set at 530 nm, using a 5 nm slit, in

four separate experiments. The extent of the lipids' contribution to any given signal was evaluated from readings observed when unlabeled peptides were titrated with lipid vesicles and subtracted as background from the recorded fluorescence intensities. The binding isotherms were analyzed as partition equilibria (Schwarz et al., 1986, 1987; Rizzo et al., 1987; Beschiaschvili & Seelig, 1990; Rapaport & Shai, 1991), using the following formula:

$$X_b^* = K_p^* C_f$$

where X_b^* is defined as the molar ratio of bound peptide per 60% of the total lipid, assuming that the peptides were initially partitioned only over the outer leaflet of the SUV, as has been previously suggested (Beschiaschvili & Seelig, 1990), K_p^* corresponds to the partition coefficient, while C_f represents the equilibrium concentration of free peptide in the solution. To calculate X_b, F_∞ (the fluorescence signal obtained when all the peptide is bound to lipid) was extrapolated from a double reciprocal plot of F (total peptide fluorescence) versus C_L (total concentration of lipids) (Schwarz et al., 1986). Knowing the fluorescence intensities of unbound peptide, F_0, as well as bound peptide, F, the fraction of membrane-bound peptide, f_b, could be calculated using

$$f_b = (F - F_0)/(F_\infty - F_0)$$

Having calculated the value of f_b, it is then possible to calculate C_f as well as the extent of peptide binding, X_b^*. The curves that result from plotting X_b^* versus free peptide, C_f, are referred to as the conventional binding isotherms.

Resonance Energy Transfer Measurements. Fluorescence spectra were obtained at room temperature on a Perkin-Elmer LS-50B spectrofluorometer, with the excitation monochromator set at 467 nm with a 5−8 nm slit width. Measurements were performed in a 0.5-cm path-length glass cuvette in a final reaction volume of 0.4 mL. To ensure proper mixing of the donor and acceptor peptides in the PC dispersion, the following technique was used. To obtain fluorescence spectrum of the donor before addition of the acceptor, the donor peptide (final concentration 0.06 μM) was added to a concentrated dispersion of PC SUV in buffer and sonicated briefly (5 s); then the dispersion was diluted to the final reaction volume and sonicated briefly again, and the spectrum was obtained. To obtain the spectrum after addition of acceptor peptide, the procedure was repeated, but this time acceptor peptide (final concentration 0.05−0.1 μM) was added to the donor peptide and the dispersion sonicated briefly before the dilution to the final reaction volume.

The efficiency of energy transfer (E) was determined by the decrease in the quantum yield of the donor as a result of the addition of acceptor. E was determined experimentally from the ratio of the fluorescence intensities of the donor in the presence (I_{da}) and in the absence (I_d) of the acceptor at the emission wavelength of the donor, after correcting for membrane light scattering and the contribution of the emission of the acceptor. The percentage value of E is given in

$$E = (1 - I_{da}/I_d) \times 100$$

The correction for light scattering was made by subtracting the signal obtained when unlabeled analogues, at concentrations equal to the sum of the donor and the acceptor, were added to vesicles. Correction for the contribution of acceptor emission was made by subtracting the signal produced by the acceptor-labeled analogue alone.

Enzymatic Digestion of Membrane-Bound S4. The ability of proteinase K to digest membrane-embedded NBD-S4 (0.05 μM) was measured in the presence and absence of 0.2 μM S3. The mixing of the peptides with the PC dispersion (final concentration 400−500 μM) was achieved as described in the preceding paragraph. Proteinase K (1 mg) was then added. Fluorescence intensities as a function of time were obtained before and after the addition of the enzyme. Fluorescence spectra were obtained at room temperature on a Perkin-Elmer LS-50B spectrofluorometer, with the excitation monochromator set at 467 nm with a 10 nm slit width, and with emission set at 530 nm with a 8 nm slit width.

RESULTS

Synthesis and Fluorescence Labeling of Peptides. In order to further characterize segments comprising the core region of the Shaker potassium channel, and the interactions between them, peptides comprising the putative transmembrane S4 and S3 segments of the Shaker potassium channel (amino acids 358−383 and 304−332, respectively) were synthesized by a solid-phase method and fluorescently labeled. S3 was extended seven amino acids toward the N-terminus relative to the consensus sequence in order to improve its solubility. Previously synthesized peptides corresponding to the S2 segment of the Shaker potassium channel (Peled & Shai, 1994) and the S4 segment from the first repeat of the eel sodium channel (Rapaport et al., 1992) were also utilized. Selective fluorescence labeling on the N-terminal amino acid of the peptides was used. The fluorophores were either NBD, which served as an environmentally sensitive probe and as a donor in RET experiments, or Rho, which served as an acceptor in RET experiments. The sequences and designations of the peptides and their analogues are presented in Table 1.

Secondary Structure Determination Using CD Spectroscopy. The extent of the α-helical secondary structure of S3 and S4 in a hydrophobic environment was estimated from their CD spectra in 40% TFE and in a membrane mimetic environment of sodium dodecyl sulfate (SDS) micelles (Figure 1). The extent of the α-helical secondary structure of S2 in 40% TFE and in SDS micelles was estimated previously (Peled & Shai, 1994). S3 did not dissolve well in 35 mM SDS solution in the relatively high concentrations needed for CD measurements ($\sim 10^{-5}$ M in comparison to $\sim 10^{-7}$ M needed for the fluorescence measurements). Therefore, it was first dissolved in TFE, and then the SDS solution was added. The total concentration of TFE was less then 10%, while conformational transition is expected to occur only at higher concentrations of TFE (Rizo et al., 1993). S4 exhibited mean residual ellipticities $[\theta]_{222}$ of −17 250 and −15 550 deg·cm^2/dmol in 40% TFE and in 35 mM SDS, respectively (Figure 1A). These values correspond to relatively high fractional helicities of 51% and 45% in the TFE and SDS solutions, respectively (Wu et al., 1981). The relatively high α-helical contents match the results obtained by Haris et al., 1994 who used FTIR

Table 1: Amino Acid Sequences of the Peptides and Their Fluorescently Labeled Analogues

no.	designation[a]	sequence[b]
1	S2 (**X** = H)	**X**-HN-^{275}I T D P F F L I E T L C I I W F T F E L T V R F L A^{300}-COOH
2	NBD-S2 (**X** = NBD)	
3	Rho-S2 (**X** = Rho)	
4	S3 (**X** = H)	**X**-HN-^{304}K L N F C R D V M N V I D I I A I I P Y F I T L A T V V A^{332}-COOH
5	NBD-S3 (**X** = NBD)	
6	Rho-S3 (**X** = Rho)	
7	S4 (**X** = H)	**X**-HN-^{358}L A I L R V I R L V R V F R I F **K** L S **R** H S K G L Q^{383}-COOH
8	NBD-S4 (**X** = NBD)	
9	Rho-S4 (**X** = Rho)	
10	S4(Na) (**X** = H)	**X**-HN-^{210}R T F R V L R A L K T I **T** I F **P** G L K T I V R A^{233}-COOH
11	NBD-S4(Na) (**X** = NBD)	
12	Rho-S4(Na) (**X** = Rho)	

[a] NBD, 7-nitrobenz-2-oxa-1,3-diazole-4-yl; Rho, tetramethylrhodamine. [b] Amino acids numbering were taken from Shaker potassium channel and the eel sodium channel.

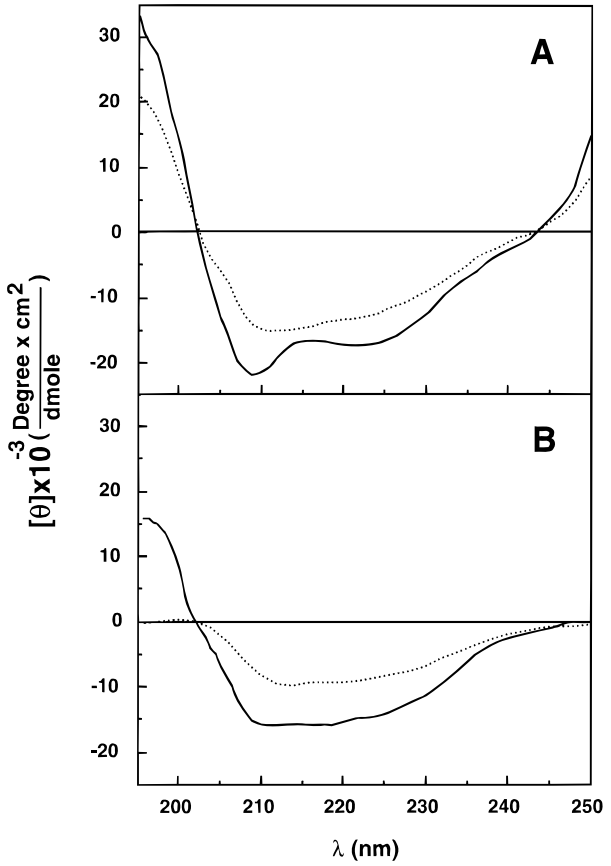

FIGURE 1: CD spectra of S3 and S4. Spectra were taken as described in Materials and Methods at peptide concentrations of $0.7-2.3 \times 10^{-5}$ M: (A) spectra taken in 40% TFE; (B) spectra taken in 35 mM SDS. (—) S4; (···) S3.

measurements in phospholipid vesicles. S3 exhibited mean residual ellipticities $[\theta]_{222}$ of −12 150 and −9400 deg·cm^2/dmol in 40% TFE and in 35 mM SDS, respectively (Figure 1B). These values correspond to lower fractional helicities of 34% and 25% in TFE and SDS, respectively.

Orientation of S3 and S4 in Phospholipid Membranes. Polarized ATR-FTIR can be used to determine the relative orientation of α-helices in oriented membranes by measuring the dichroism of the amide I vibrational mode of the α-helix. The CD measurements of S4 shows that it contains a significant amount of α-helical structure (about 50%); therefore, ATR-FTIR might be used to gain some information about its orientation in membranes. Regarding S3, its lower

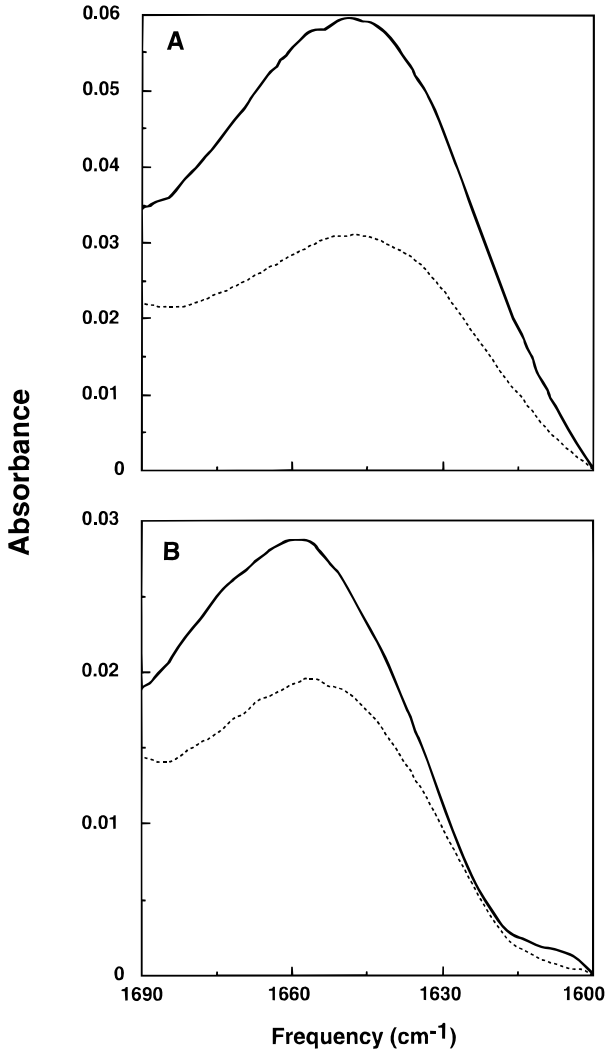

FIGURE 2: ATR-FTIR spectra of S3 and S4 in DMPC. The polarized ATR-FTIR spectra of S3 (A) and S4 (B) were obtained using parallel (solid line) or perpendicular (dotted line) polarized light.

helical content makes ATR-FTIR results less conclusive. Figure 2 presents the ATR-FTIR spectra of S3 and S4 obtained with parallel and perpendicular polarized light. Table 2 lists the measured dichroic ratios, derived order parameters, and corresponding tilt angles for S3 and S4 in DMPC. In these measurements, the lipid vibrations serve as internal standards for estimating the overall orientation of the membranes. The average order parameters obtained

Table 2: ATR-FTIR Dichroic Ratios, Order Parameters, and Calculated Tilt Angles

	lipid chain		peptide α-helix			
peptide	R^{ATR}	S	amide I (cm^{-1})	R^{ATR}	S	tilt angle (θ)
S3	0.99	0.83	1650	2.35	0.23	49°
S4	0.96	0.86	1658	1.60	−0.32	70°

for the lipid methylene symmetric (2852 cm^{-1}) and asymmetric (2924 cm^{-1}) stretching modes are S_{lipid} $CH_2 = 0.83$ and 0.86 for S3 and S4 measurements, respectively. These order parameters indicate that the membranes are well-oriented (Smith et al., 1994). Order parameters for overall membrane orientation ($S_{membrane} = 0.87$ and 0.90 for S3 and S4 measurements, respectively) can be defined based on the lipid order parameter by accounting for a 10° tilt of the lipid acyl chains in gel phase membranes (Hauser et al., 1981).

The observed dichroic ratios and corresponding helix order parameters for S3 ($R^{ATR} = 2.35$, $S_{helix} = 0.23$) and S4 ($R^{ATR} = 1.6$, $S_{helix} = -0.32$) correspond to those observed for the most well-ordered peptides and translate into tilt angles of 49° for S3 and 70° for S4. These values are obtained by assuming that the membranes are perfectly oriented ($S_{membrane} = 1.0$) parallel to the surface of the internal reflection element and that the helix order parameters result entirely from a tilt away from the bilayer normal. Assuming that the helix order parameters result from a combination of helix tilt and membrane disorder, a correcting factor can be introduced ($1/S_{membrane} = 1.15$ and 1.11 for S3 and S4 measurements, respectively) which accounts for disorder in membrane orientation. The tilt angles derived for S3 and S4 in this manner are 44° and 72°, respectively. In other words, S4 is oriented almost parallel to the membrane plane. As for S3, its tilt angle suggest a transmembrane orientation.

NBD Fluorescence Measurements. To determine qualitatively the ability of S3 and S4 to partition into phospholipid membranes, NBD-labeled peptide analogues were utilized. The NBD group has been widely used for polarity and binding studies, because it is sensitive to the dielectric constant of its environment (Kenner & Aboderin, 1971; Frey & Tamm, 1990; Baidin & Huang, 1990; Rapaport & Shai, 1991). Thus, it is possible to correlate changes in the emission spectra of NBD with changes in the hydrophobicity of its environment. The fluorescence emission spectra of NBD-S3 and NBD-S4 were measured in aqueous solution and in the presence of PC vesicles. When placed in buffer, NBD-S3 and NBD-S4 exhibited a fluorescence emission maxima at 540 ± 4 and at 545 ± 3 nm, respectively, and a low quantum yield in their fluorescence intensity (Figure 3A,B), in agreement with the reported emissions for NBD derivatives placed in hydrophilic solutions (Rajarathnan et al., 1989; Rapaport & Shai, 1991). However, when added to a solution of PC vesicles (pH 6.8), the N-terminally labeled peptides exhibited enhanced increases in their fluorescence intensity and a blue-shift in their fluorescence emission maxima (Figure 3A,B). The emission maxima now were 527 ± 2 and 532 ± 1 for NBD-S4 and NBD-S3, respectively. These changes reflect the relocation of the NBD groups into a more hydrophobic environment (Chattopadhyay & London, 1987). The blue-shift of S4 in PC suggests that the N-terminus of the peptide is buried not deeply within the phospholipid membranes (Rapaport & Shai, 1992; Gazit & Shai, 1993b). The blue-shift of S3, on the other hand,

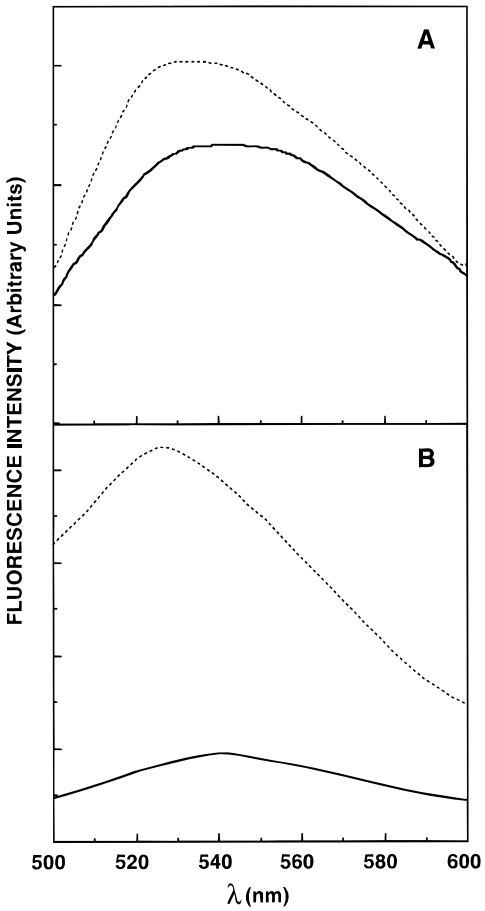

FIGURE 3: Fluorescence emission spectra of NBD-labeled S3 and S4. Spectra were determined in the presence or absence of SUV vesicles in buffer composed of 50 mM Na_2SO_4 and 23 mM HEPES/SO_4^{2-} (pH 6.8). The excitation wavelength was set at 467 nm, and emission was scanned from 500 to 600 nm. (A) 0.2 μM NBD-S3 in the absence (filled line) or presence (dotted line) of 800 μM PC vesicles. (B) 0.1 μM NBD-S4 in the absence (filled line) or presence (dotted line) of 300 μM PC vesicles.

resembles that observed for an NBD group located at or near the surface (emission maximum of 530−534) (Chattopadhyay & London, 1987; Rajarathnan et al., 1989; Pouny et al., 1992). The S3 peptide included seven amino acids from the cytoplasmic loop S2−S3 in order to improve its solubility. As the NBD moiety is attached to the N-terminal amino acid, the surface localization might be due to this elongation rather than point to the localization of the S3 segment itself. In these experiments, the lipid/peptide molar ratio was consistently maintained at elevated levels (2400−3000:1) so that the spectral contributions of free peptide would be negligible.

Binding Experiments. The next step was to determine more quantitatively the affinity of the peptides to phospholipid membranes. To that end the surface partition coefficients of S3 and S4 between phospholipid membranes and buffer were determined. Knowing the surface partition coefficients of the peptides is necessary to ensure that all or most of the peptides are bound to membranes under the conditions of the RET experiments. The environment-sensitive NBD moiety was used again, and samples of NBD-labeled peptides (0.1−0.2 μM) were mixed with increasing amounts of PC vesicles, at pH 6.8. The increases in the fluorescence intensities of the NBD-labeled S4 or S3 were plotted as a function of the lipid/peptide molar ratios to form

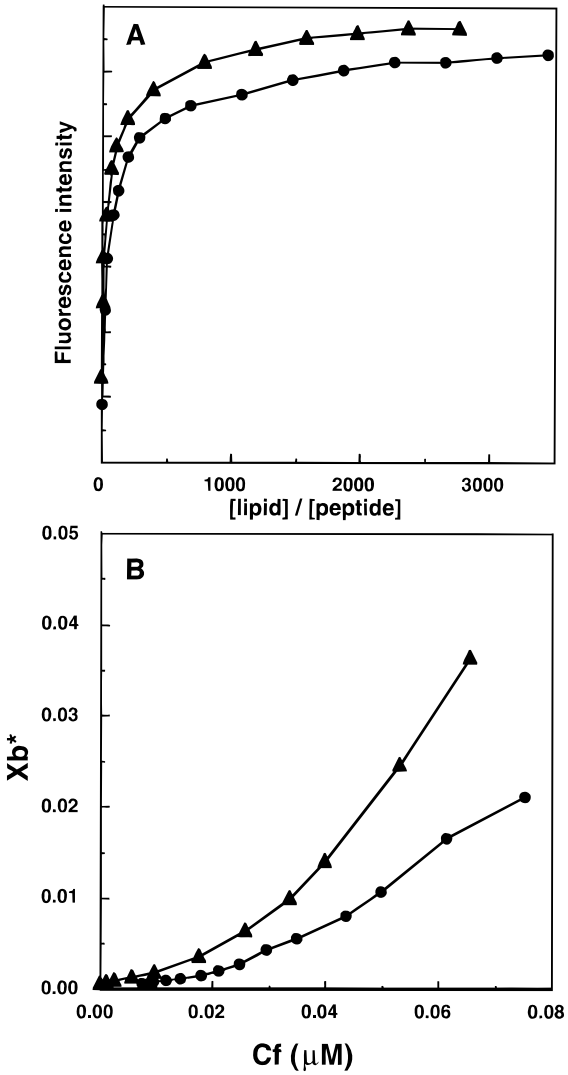

FIGURE 4: Increases in the fluorescence of NBD-S3 and NBD-S4 upon titration with PC vesicles (A), and the resulting binding isotherm (B). 0.2 μM NBD-S3 (circles) or 0.1 μM NBD-S4 (triangles) were titrated with PC SUV with excitation set at 467 nm and emission recorded at 530 nm. The experiment was performed at room temperature in 50 mM Na_2SO_4 and 25 mM HEPES-SO_4^{2-}, pH 6.8. The binding isotherm was derived from panel A by plotting X_b* (molar ratio of bound peptide per 60% lipid) versus C_f (equilibrium concentration of free peptide in the solution).

binding curves (see panel A in Figure 4). Similar results were obtained whether the vesicles were added successively to a solution containing the peptide or whether a fixed amount of peptide was added to separate cuvettes containing increasing amounts of vesicles. Therefore (and because of the low concentrations of peptides used in this experiment), it was assumed that the peptides are not aggregated in the solution before the addition of lipid vesicles. Since the concentration of NBD-peptide in the mixture was low, the peptide was also assumed not to disrupt the bilayer structure. When unlabeled peptide was titrated with lipids up to the maximal concentration used with NBD-peptide, the fluorescence intensities of the solution, after subtracting the contribution of the vesicles, remained unchanged.

The binding isotherms were analyzed as partition equilibria as described in Material and Methods. The curves obtained by plotting X_b* (the molar ratio of bound peptide per 60% of the total lipid assumed to be in the outer leaflet) versus C_f (the equilibrium concentration of free peptide in the solution), referred to as the conventional binding isotherms, are shown in panel B in Figure 4. The surface partition coefficients, K_p*, were estimated by extrapolating the initial slopes of the curves to zero C_f values. The K_p* values are $3.6 \pm 2.2 \times 10^4$ M^{-1} and $1.8 \pm 0.7 \times 10^5$ M^{-1} for S3 and S4, respectively (means of four different experiments). These K_p* values are within the range of those obtained for membranous bioactive peptides, such as melittin and its derivatives (Stankowski & Schwarz, 1990), the *Staphylococcus* δ-toxin (Thiaudière et al., 1991), the antibiotic dermaseptin (Pouny et al., 1992), and pardaxin and its analogues (Rapaport & Shai, 1991).

The shape of the binding isotherms of S3 and S4 deviate somewhat from linearity, but they do not display the sharp rise that is typical to a cooperative binding process. Thus, the pronounced aggregational state that is evident from the binding isotherms of several membrane bound peptides such as alamethicin (Rizzo et al., 1987), the shark repellent neurotoxin, pardaxin (Rapaport & Shai, 1991, 1992), and the α5 segment of *Bacillus thuringiensis* δ-endotoxin (Gazit & Shai, 1993a) does not exist in S3 and S4.

Resonance Energy Transfer (RET) Experiments. In light of earlier results showing that membrane-embedded segments from the Shaker potassium channel are able to self-associate and to associate with each other in their membrane-bound state (Peled & Shai, 1993, 1994), we decided to check the ability of S4 and S3 to self-associate or to form heteroaggregates with each other or with the S2 segment. RET measurements were performed as described in Materials and Methods utilizing NBD-labeled peptides as energy donors and Rho-labeled peptides as energy acceptors (Table 1). In these experiments zwitterionic PC phospholipid vesicles were used to prevent a contribution of the lipid head group charge to the binding process, and low peptide/lipid molar ratios were maintained. Energy transfer from donor-labeled peptide to acceptor-labeled peptide is apparent when the donor's emission is quenched and the acceptor's emission is increased relative to what is expected from random distribution of the peptides in the phospholipid membranes. Examples of typical profiles of the energy transfer from NBD-S2 to Rho-S3, in the presence of phospholipid vesicles, are depicted in Figure 5A, and those showing the energy transfer from NBD-S3 to Rho-S3, in the presence of phospholipid vesicles, are depicted in Figure 5B. It can be clearly seen that the addition of Rho-S3 (final concentrations of 0.05−0.1 μM) to NBD-S2 (0.06 μM), but not to NBD-S3, with phospholipid vesicles (160 μM) significantly quenched the donor's emission and increased the acceptor's emission, which is consistent with energy transfer. Similar experiments were done with combinations of the peptides.

To determine the actual percentage of energy transfer, the amounts of lipid-bound acceptors (Rho-peptides, termed "bound acceptor") at the various acceptor-peptide concentrations were calculated from the binding isotherms of the corresponding NBD-labeled peptides as previously described (Pouny et al., 1992). The curves of the experimentally derived percentage of energy transfer versus the bound acceptor/lipid molar ratios are depicted in Figure 6. Only the bound acceptor/lipid molar ratios are used, as the energy transfer efficiency is independent of the surface density of the donor (Fung & Stryer, 1978), and as the lipid/donor ratio was kept constant in all of the experiments. A curve corresponding to random distribution of monomers (Fung

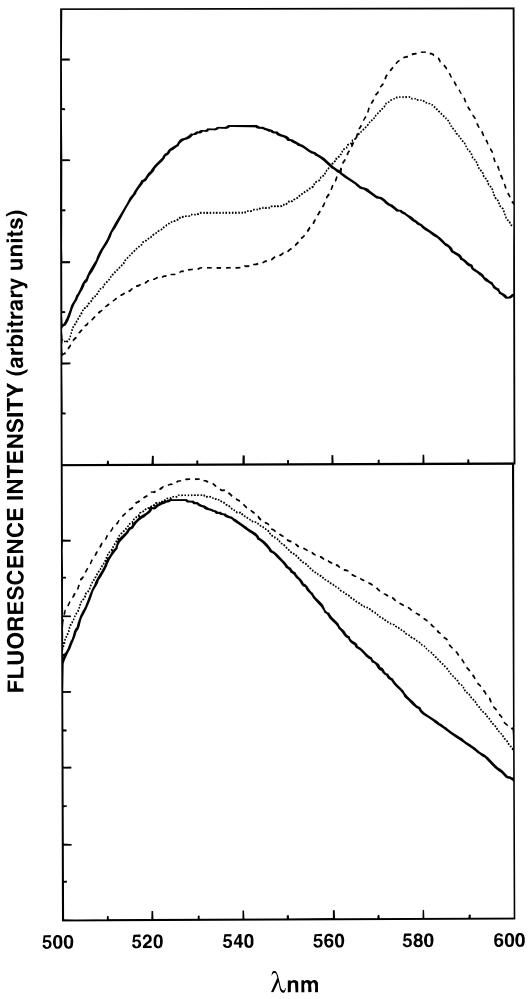

FIGURE 5: Fluorescence energy transfer dependence on Rho-peptide (acceptor) concentration. The spectrum of donor-peptide, either NBD-S2 (panel A) or NBD-S3 (panel B), was determined in the absence or presence of various concentrations of acceptor peptide, Rho-S3. Each spectrum was recorded in the presence of 160 μM PC SUV in 50 mM Na_2SO_4 and 25 mM HEPES-SO_4^{2-}, pH 6.8. The excitation wavelength was set at 467nm; emission was scanned from 500 to 600 nm. The spectrum of Rho-S3 in the presence of vesicles and unlabeled donor peptide was subtracted from each spectrum. (A) (—) 0.06 μM NBD-S2; (•••) a mixture of 0.06 μM NBD-S2 and 0.05 μM Rho-S3; (- - -) a mixture of 0.06 μM NBD-S2 and 0.1 μM Rho-S3. (B) (—) 0.06 μM NBD-S3; (•••) a mixture of 0.06 μM NBD-S3 and 0.05 μM Rho-S3; (- - -) a mixture of 0.06 μM NBD-S3 and 0.1 μM Rho-S3.

& Stryer, 1978), assuming a R_0 of 51 Å, which was previously calculated for the NBD/Rho donor/acceptor pair (Gazit & Shai, 1993b), is also depicted. A high percentage of energy transfer, and therefore association, was obtained with NBD-S2/Rho-S4, NBD-S2/Rho-S3, NBD-S3/Rho-S4, and their reciprocal pairs (Figure 6). These values are markedly higher than those that would be obtained if the distribution of monomers was assumed to be random. However, the efficiency of energy transfer between NBD-S4/Rho-S4, NBD-S3/Rho-S3, NBD-S3/Rho-S4(Na), and NBD-S4(Na)/Rho-S3 was not significantly different from that observed for random distribution (Figure 6). Thus, although S4 and S3 were not able to self-associate, they did associate with each other and with the S2 segment of the channel rather than distribute randomly throughout the phospholipid membranes. Furthermore, S3 was able to coassemble with the S4 of the Shaker K^+ channel, but not with the homologous S4 segment of the Na^+ channel. Thus,

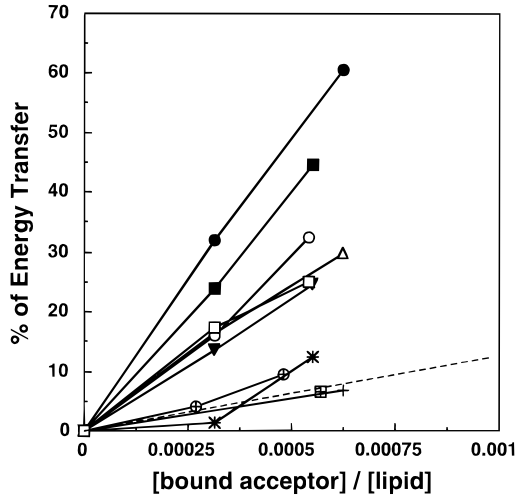

FIGURE 6: Theoretically and experimentally derived percentages of energy transfer versus bound acceptor/lipid molar ratio. The amount of lipid-bound acceptor (Rho-peptides), C_b, at various acceptor concentrations was calculated from the binding isotherms. First, the fractions of bound acceptor, f_b, were calculated for the various peptide/lipid molar ratios from their binding isotherms and were then used to calculate the amount of bound acceptor (Pouny et al., 1992). Symbols: filled squares, NBD-S2/Rho-S3; open squares, NBD-S3/Rho-S2; filled triangles, NBD-S4/Rho-S3; open triangles, NBD-S3/Rho-S4; filled circles, NBD-S2/Rho-S4; open circles, NBD-S4/Rho-S2; crosses, NBD-S4/Rho-S4; crossed circles, NBD-S3/Rho-S3; crossed squares, NBD-S3/Rho-S4(Na); crossed X, NBD-S4(Na)/Rho-S3; dashed line, random distribution of the monomers (Fung & Stryer, 1978), assuming an R_0 of 51 Å.

some specificity exist in these interactions. It should be noted that the peptide/lipid molar ratio range in which the RET experiments were done (0.0003−0.0006) is about one order of magnitude lower than the peptide/lipid molar ratio at which a deviation from linearity was noticed in the binding experiments of S3 and S4 to PC vesicles (0.002−0.006). Hence, if any aggregation occurs, it will only take place at much higher peptide/lipid molar ratio.

Enzymatic Digestion of Membrane-Bound S4. The RET measurements demonstrated that S4 is able to associate with S3. The enzymatic digestion experiments were aimed at checking whether the interactions between S3 and S4 can influence the position of S4 in the membrane. When proteinase K was added to membrane-bound NBD-S4, a small decrease in the fluorescence of the NBD moiety was observed (Figure 7). This decrease is due to digestion of the peptide or its N-terminal, which causes the release of some of the NBD into the hydrophilic solution, consequently decreasing its fluorescence. As can be clearly seen, only a small percentage of the NBD is initially released into the solution, and the kinetics of the digestion is slow. These results support the notion that most of the N-terminal of S4 is found in the phospholipid milieu, as was determined in the NBD fluorescence experiments. When proteinase K was added to a mixture of membrane-bound NBD-S4 and S3, the initial kinetic of the digestion was steeper, and more of the NBD-S4 seemed to be digested (Figure 7). This change reflect a change in the position of NBD-S4 in the membrane due to interactions with S3. This change increased the lability of the N-terminal of the peptide to enzymatic cleavage. The fact that the fluorescence of NBD-S4 in the presence of S3 was higher than its fluorescence without S3 (Figure 7) further supports a change in the position of NBD-S4 as a result of interactions between the peptides.

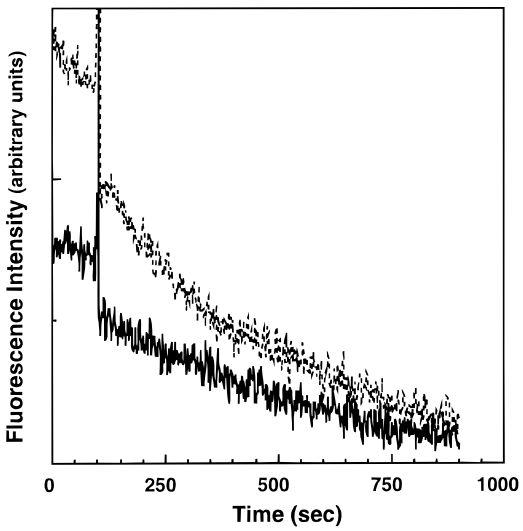

FIGURE 7: Digestion of membrane-bound NBD-S4 by proteinase K. The fluorescence of NBD-S4 (0.05 μM) as a function of time, before and after the addition of Proteinase K (1 μg), was determined in the absence (full line) or presence (dashed line) of S3 (0.2 μM). Proteinase K was added at time = 100 s. Each spectrum was recorded in the presence of 400−500 μM PC SUV in 50 mM Na_2-SO_4, 25 mM HEPES-SO_4^{2-}, pH 6.8 (final volume 400 μL).

DISCUSSION

Increasing evidence suggest that membrane-embedded segments can interact within the phospholipid milieu of the membrane in varying degrees of specificity, and thus contribute to the folding and oligomerization of the proteins [see review by Lemmon and Engelman (1994)]. We have used the S4 segment of the Shaker potassium channel and its neighboring segments, S2 and S3, as a case study that enabled us to look at interactions between membranous segments. The elucidation of such interactions is important not only to the understanding of the assembly and organization of the potassium channel protein but also to improve our understanding of the general rules that are involved in the interactions between transmembrane segments of membrane proteins.

The existence of a positive charge at every third or fourth position and the conservation of the S4 segment within voltage-gated ion channels have led to the idea that S4 is the voltage sensor of these channels. It is assumed that the positive charges on S4 are neutralized by interactions with negative charges on other segments from the core region of the channel (Greenblatt et al., 1985; Montal, 1990). Moreover, cGMP- and cAMP-gated ion channels, which are not voltage sensitive, have segments homologous to S4, therefore suggesting that there are other structural roles to this region. Hence, it is interesting to look not only at the involvement of the S4 segment in the voltage-dependent activation of the channel but also at its interactions with other components of the pore and at its role as a structural component of the channel.

Recently, several groups have proposed that S4 alone cannot account for the voltage dependence of the channel, and that acidic residues in the S2 and S3 segments might also be involved in the voltage sensing of the channel (Koopmann et al., 1995; Ledwell et al., 1995; Papazian et al., 1995; Planelles-Cases et al., 1995; Seoh & Papazian, 1995). These acidic residues might form electrostatic interactions with positive charges on the S4 segment (Bezanilla et al., 1995; Papazian et al., 1995; Planelles-Cases et al., 1995). Our resonance energy transfer experiments clearly show that the S4 segment can indeed interact with either the S2 or the S3 segments (Figure 6), and thus they support this hypothesis. On the other hand, S3 does not interact with the S4 segment from the eel sodium channel (Figure 6). Two positively charged amino acids in S4 were shown to interact with negatively charged amino acids in S2 and S3 [K374 and R377 (Papazian et al., 1995)]. Both of them do not have homologous positive charges in the S4 from the sodium channel (see Table 1, the discussed amino acids are given in bold letters). Thus, it is tempting to assume that the lack of those necessary residues prevent the coassembly of S3 and the S4 segment of the sodium channel. Of course, there are probably other residues which play part in the interactions between S4 and either S2 or S3 (Planells-Cases et al., 1995).

The energy transfer experiments also demonstrated a degree of specificity in the interactions of the different segments of the Shaker potassium channel. Neither S3 nor S4 can self-associate in zwitterionic vesicles at low peptide/lipid molar ratios. S4 is highly positively charged; therefore, it is reasonable to assume that in zwitterionic phospholipids these charges are not masked, and therefore electrostatic repulsion prevent interaction. It is also reasonable to assume that electrostatic interactions play important role in the interaction between the positively charged S4 and the negatively charged S2. On the other hand, as was shown for the interactions between the H5 and the S2 segments (Peled & Shai, 1994), electrostatic interactions cannot be the only force that drives the interactions between the different segments. The S3 peptide carries one negative charge, and although it does not self-associate, it is able to associate with the S2 segment which carries three negative charges. Thus, the interactions between S2 and S3 exist in spite of their negative charges.

Hydropathy plots and modeling studies predicted that both the S4 and the S3 segments are membrane spanning and α-helical (Durell & Guy, 1992). Our CD measurements (Figure 1) as well as recent results of FTIR and CD studies by Haris et al. (1994) confirm the α-helical content of S4. Similar results were obtained by 2D NMR studies on the S4 segment of the first internal repeat of the rat brain sodium channel (Mulvey et al., 1989). It is interesting to note that although the S4 of the first internal repeat of the sodium channel contains proline while the S4 of the potassium channel does not, the α-helical contents of these two segments are similar. As for the S3 segment, our CD measurements reveal a lower degree of α-helical content (Figure 1). Similar results were obtained with the S3 segment of repeat I from rat brain sodium channel I (Oiki et al., 1990). The S3 peptide that was used included seven amino acids (or 25% of its length) in addition to the consensus S3 sequence, in order to improve its solubility. These extra amino acids, not belonging to the predicted α-helix, could reduce the actual α-helical content of the S3 sequence itself. Thus, the actual α-helical content might be at least ∼25% higher, namely, about 40% and 32% in TFE and SDS, respectively. Furthermore, S3 contains proline in its sequence. Proline is known to induce kinks in transmembrane helices, the presence of such a kink might reduce the α-helical content observed by CD measurements. Our

results and those of Harris et al. (1994) demonstrate that S4 retains its α-helical structure in three different hydrophobic environments, TFE, SDS, and phospholipids, demonstrating the stability of its structure. Similar results have been shown in several other cases of membrane interacting segments (Shai et al., 1991; Gazit et al., 1993b; Li & Deber, 1994). Taken together with the results of recent studies that have shown that various synthetic segments from bacteriorhodopsin (Barsukov et al., 1992) and from the pore region of δ-endotoxin (Gazit & Shai, 1993a) adopt α-helical conformations similar to those of the relevant segments within the intact protein as determined by cryoelectron and X-ray crystallography, it might be that S4, as well as S3, retains similar structure in the native channel.

The role of S4 as the voltage sensor of the channel requires it to be flexible and sensitive to its environment. The current model predicts that in order for a channel to open in response to voltage change, its four S4 segments must move from a nonpermissive to a permissive position. Indeed, recent studies have demonstrated movement of at least several residues of the S4 segment, either in the potassium channel or in the sodium channel, in response to changes in membrane potential (Mannuzzu et al., 1996; Yang et al., 1996). Thus, the S4 segments have more then one energetically stable position, and their position is dependent on the environment. The ATR-FTIR results indicate that S4 is located on the surface of the membrane. Therefore, it seems that S4 needs its surrounding segments and/or membrane potential in order to assume transmembranal position and is indeed stable in other positions as well. The enzymatic cleavage experiments (Figure 7) demonstrate that the presence of S3 indeed induce some change in the position of the S4 segment, though the exact nature of this change can not be deduced from the present data. The orientation of S3, on the other hand, was found to be closer to the expected transmembranal orientation. As S3 is only partially helical, the other secondary structures present are expected to reduce its order parameter in membranes. Thus, the calculated tilt angle does not represent solely the orientation of the peptide, and the true tilt angle is probably lower then the observed one (Frey & Tamm, 1991).

The NBD fluorescence measurements as well as the binding experiments indicate strong interactions between the S3 or the S4 segments and zwitterionic phospholipid membranes (Figures 3 and 4). Similar results were shown with the S4 derived from the first repeat of the eel sodium channel (Rapaport et al., 1992). S4 demonstrates unexpectedly high partition coefficient to neutral phospholipids, being one order of magnitude higher than the partition coefficient of similarly positively charged peptides such as the antibacterial peptides dermaseptin (Pouny et al., 1992) and cecropin B2 (Gazit et al., 1994). The high affinity of S4 for phospholipid membranes is surprising in light of its high positive charge. This might reflect the importance of hydrophobic interactions between S4 and its surroundings. In support of this, mutation experiments in S4 implied that hydrophobic interactions indeed occur between S4 and its immediate surroundings (which might be either other segments of the channel or the surrounding lipids), and that these interactions have functional importance (Lopez et al., 1991). Furthermore, the ability of S4 to interact with phospholipid membranes is in accordance with the "two stage" model for membranal protein folding and oligomerization (Popot et al., 1987; Popot & Engelman, 1990). In this "two stage" model, the final structure in membranes results from the packing of smaller elements, each of which reaches thermodynamic equilibrium with the lipid and aqueous phases before packing. The model excludes structures incorporating transmembrane segments that are not individually stable in the membrane. Thus, S4 is able to interact strongly with the phospholipid membranes by itself, while its proper orientation in the membranes probably requires the framework of its neighboring segments. Recently, it was demonstrated that expression of bovine opsin gene fragments from rhodopsin leads to production of stable polypeptide fragments. Coexpression of two or three complementary fragments results in assembly of rhodopsin which appears to have the native structure *in vivo*, though not necessarily having native function (Ridge et al., 1995). Such experiments strengthen the notion that fragments of membrane proteins can adopt their native structure and position as implicated from the two-stage model (Popot et al., 1987; Popot & Engelman, 1990) and thus support the notion that results obtained with individual segments of a protein are applicable to its native structure.

Finally, according to models, S2 and S4 should be parallel to each other and antiparallel to S3 in the assembled complex in the membrane. With regard to S4, recent studies have shown that its position in potassium, as well as sodium channels, is dynamic, and that depolarization of the membrane cause movement of several amino acids of the S4 segment to the extracellular environment (Mannuzzu et al., 1996; Yang et al., 1996). Thus, the orientation of S4 in the isolated model system of two segments in the membrane would not be expected to reflect the complexity of the whole channel. However, there are good reasons to assume that the isolated segments are indeed assembled in the correct orientation. First, as was shown S3 assembles specifically with the S4 of the Shaker K^+channel but not with the S4 of the sodium channel. This is probably due to lack of two positively charged amino acids at the C-terminal part of the S4 of the sodium channel that were shown to interact with negatively charged amino acids in the C-terminal part of S2 and the N-terminal part of S3 [K374 and R377 (Papazian et al., 1995)]. Secondly, it was found that in vitro assembly of separated transmembrane helices occurs within a bilayer environment and lead to the formation of functional proteins (Liao et al., 1984; Popot et al., 1987; Kahn & Engelman, 1992), and that several isolated transmembrane helices are assembled as is expected from their position in the intact protein. The list includes the parallel organization of α-5 (Gazit & Shai, 1995), and the antiparallel organization of α-4 and α-5 of the *B. thuringiensis* CryIIIA δ-endotoxin.[2] Studies are being conducted to determine the exact orientation of the helices studies herein.

In summary, we have shown that interactions exist between synthetic peptides resembling the S2, S3, and S4 segments of the Shaker potassium channel. These results correlate with previous data suggesting that S4 alone cannot account for the voltage dependence of the channel, and that acidic residues in the S2 and S3 segments might also be involved in the voltage sensing of the channel (Koopmann et al., 1995; Ledwell et al., 1995; Papazian et al., 1995; Planelles-Cases et al., 1995). The interactions between S4 and S2 or S3 are

[2] E. Gazit and Y. Shai (1996) 24th Meeting of the Federation of Biochemical Societies (FEBS), Aug 7−12, 1996, Barcelona, Spain.

not necessarily based solely on the attraction of opposite charges, as it was shown that S4 is able to interact strongly with neutral environment such as zwitterionic phospholipids. Those results should be looked at from a broader point of view, as there is an increasing body of data suggesting that specific and nonspecific interactions between transmembrane segments play an important role in membrane proteins folding, assembly, and function [see review by Lemmon and Engelman (1994)].

REFERENCES

Babila, T., Moscucci, A., Wang, H., Weaver, F. E., & Koren, G. (1994) *Neuron 12*, 615−626.

Baidin, G., & Huang, J. R. (1990) *FEBS Lett. 259*, 254−256.

Barsukov, I. L., Nolde, D. E., Lomize, A. L., & Arseniev, A. S. (1992) *Eur. J. Biochem. 206*, 665−672.

Bartlett, G. R. (1959) *J. Biol. Chem. 234*, 466−468.

Ben-Efraim, I., Bach, D., & Shai, Y. (1993) *Biochemistry 32*, 2371−2377.

Beschiaschvili, G., & Seelig, J. (1990) *Biochemistry 29*, 52−58.

Bezanilla, F., Seoh, S.-A., & Papazian, D. M. (1995) *Biophys. J. 68*, A137.

Catterall, W. A. (1988) *Science 242*, 50−61.

Chattopadhyay, A., & London, E. (1987) *Biochemistry 26*, 39−45.

Chen, Y. H., Yang, J. T., & Chau, K. H. (1974) *Biochemistry 13*, 3350−3359.

Christie, M. J., North, R. A., Osborne, P. B., Douglass, J., & Adelman, J. P. (1990) *Neuron 2*, 405−411.

Covarrubias, M., Wei, A., & Salkoff, L. (1991) *Neuron 7*, 763−773.

Durell, S. R., & Guy, H. R. (1992) *Biophys. J. 62*, 238−250.

Frey, S., & Tamm, L. K. (1990) *Biochem. J. 272*, 713−719.

Fringeli, U. P., Apell, H. J., Fringeli, M., & Lauger, P. (1989) *Biochim. Biophys. Acta 984*, 301−312.

Fung, B. K., & Stryer, L. (1978) *Biochemistry 17*, 5241−5248.

Gazit, E., & Shai, Y. (1993a) *Biochemistry 32*, 3429−3436.

Gazit, E., & Shai, Y. (1993b) *Biochemistry 32*, 12363−12371.

Gazit, E., & Shai, Y. (1995) *J. Biol. Chem. 270*, 2571−2578.

Gazit, E., Lee, W.-J., Brey, P. T., & Shai, Y. (1994) *Biochemistry 33*, 10681−10692.

Greenblatt, R. E., Blatt, Y., & Montal, M. (1985) *FEBS Lett. 193*, 125−134.

Greenfield, N., & Fasman, G. D. (1969) *Biochemistry 8*, 4108−4116.

Haris, P. I., Ramesh, B., Brazier, S., & Chapman, D. (1994) *FEBS Lett. 349*, 371−374.

Harrick, N. J. (1967) *Internal Reflection Spectroscopy*, Interscience Publishers, New York.

Hauser, H., Pascher, I., Pearson, R. H., & Sundell, S. (1981) *Biochim. Biophys. Acta 650*, 21−51.

Hille B. (1992) *Ionic Channels of Excitable Membranes*, Sinauer, Sunderland, MA

Isacoff, E. Y., Jan, Y. N., & Jan, L. Y. (1990) *Nature 345*, 530−534.

Kahn, T. W., & Engelman, D. M. (1992) *Biochemistry 31*, 6144−6151.

Kenner, R., & Aboderin, A. (1971) *Biochemistry 10*, 4433−4440.

Kirsch, G. E., Drewe, J. A., De Biasi, M., Hartmann, H. A., & Brown, A. M. (1993) *J. Biol. Chem. 268*, 13799−13804.

Koopmann, R., Benndorf, K., Lorra, C., & Pongs, O. (1995) *Biophys. J. 68*, A34.

Liao, M. J., Huang, K. S., & Khorana, H. G. (1984) *J. Biol. Chem. 259*, 4200−4204.

Ledwell, J. L., Smith-Maxwell, C. J., & Aldrich, R. W. (1995) *Biophys. J. 68*, A32.

Lemmon, M. A., & Engelman, D. M. (1994) *Q. Rev. Biophys. 27*, 157−218.

Lee, T. E., Philipson, L. H., Kuznetsov, A., & Nelson, D. J. (1994) *Biophys. J. 66*, 667−673.

Li, M., Jan, Y. N., & Jan, L. Y. (1992) *Science 257*, 1225−1230.

Li, S.-C., & Deber, C. M. (1994) *Nature, Struct. Biol. 1*, 368−373.

Liman, E. R., Tytgat, J., & Hess, P. (1992) *Neuron 9*, 861−871.

Lopez, G. A., Jan, Y. N., & Jan, L. Y. (1991) *Neuron 7*, 327−336.

MacKinnon, R. (1991) *Nature 350*, 232−235.

Mannuzzu, L. M., Moronne, M. M., & Isacoff, E. Y. (1996) *Science 271, 213*−216.

McCormack, K., Lin, J. W., Iverson, L. E., & Rudy, B. (1990) *Biochem. Biophys. Res. Commun. 171*, 1361−1371.

Merrifield, R. B., Vizioli, L. D., & Boman, H. G. (1982) *Biochemistry 21*, 5020−5031.

Montal, M. (1990) *FASEB J.*, 2623−2635.

Mulvey, D., King, G. F., Cooke, R. M., Doak, D. G., Harvey, T. S., & Campbell, I. D. (1989) *FEBS Lett. 257*, 113−117.

Oiki, S., Madison, V., & Montal, M. (1990) *Proteins: Struct. Funct., Genet. 8*, 226−236.

Papahadjopoulos, D., & Miller, N. (1967) *Biochim. Biophys. Acta 135*, 624−638.

Papazian, D. M., Timpe, L. C., Jan, Y. N., & Jan, L. Y. (1991) *Nature 349*, 305−310.

Papazian, D. M., Shao, X. M., Seoh, S.-A., Mock, A. F., Huang, Y., & Wainstock, D. H. (1995) *Neuron 14*, 1293−1301.

Peled, H., & Shai, Y. (1993) *Biochemistry 32*, 7879−7885.

Peled, H., & Shai, Y. (1994) *Biochemistry 33*, 7211−7219.

Planells-Cases, R., Ferrer-Montiel, A. V., Patten, C. D., & Montal, M. (1995) *Proc. Natl. Acad. Sci. U.S.A. 92*, 9422−9426.

Pouny, Y., Rapaport, D., Mor, A., Nicolas, P., & Shai, Y. (1992) *Biochemistry 31*, 12416−12423.

Popot, J.-L., & Engelman, D. M. (1990) *Biochemistry 29*, 4031−4037.

Popot, J.-L., Gerchman, S.-E., & Engelman, D. M. (1987) *J. Mol. Biol. 198*, 655−676.

Rajarathnam, K., Hochman, J., Schindler, M., & Ferguson-Miller, S. (1989) *Biochemistry 28*, 3168−3176.

Rapaport. D., & Shai. Y. (1991) *J. Biol. Chem. 266*, 23769−23775.

Rapaport, D., & Shai, Y. (1992) *J. Biol. Chem. 267*, 6502−6509.

Rapaport, D., Danin, M., Gazit, E., & Shai, Y. (1992) *Biochemistry. 31*, 8868−8875.

Ridge, K. D., Lee, S. S. J., & Yao, L. L. (1995) *Proc. Natl. Acad. Sci. U.S.A. 92*, 3204−3208.

Rizo, J., Blanco, F. J., Kobe, B., Bruch M. D., & Gierasch, L. M. (1993) *Biochemistry 32*, 4881−4894.

Rizzo, V., Stankowsky, S., & Schwarz, G. (1987) *Biochemistry 26*, 2751−2759.

Ruppersberg, J. P., Schröter, K. H., Sakmann, B., Stocker, M., Sewing, S., & Pongs, O. (1990) *Nature 345*, 535−537.

Schwarz, G., Stankowsky, S., & Rizzo, V. (1986) *Biochim. Biophys. Acta 861*, 141−151.

Schwarz, G., Gerke, H., Rizzo, V., & Stankowsky, S. (1987) *Biophys. J. 52*, 685−692.

Shai, Y., Bach, D., & Yanovsky, A. (1990) *J. Biol. Chem. 265*, 20202−20209.

Shen, N. V., Chen, X., Boyer, M. M., & Pfaffinger, P. J. (1993) *Neuron 11*, 67−76.

Smith, S. O., Jonas, R., Briaman, M. S., & Bormann, B. J. (1994) *Biochemistry 33*, 633−641.

Stankowsky, S., & Schwarz, G. (1990) *Biochim. Biophys. Acta 1025*, 164−172.

Taglialatela, M., Champagne, M. S., Drewe, J. A., & Brown, A. M. (1994) *J. Biol. Chem. 269*, 13867−13873.

Tamm, L. K., & Tatulian, S. A. (1993) *Biochemistry 32*, 7720−7726.

Thiaudière, E., Siffert, O., Talbot, J. C., Bolard, J., Alouf, J. E., & Dufourcq, J. (1991) *Eur. J. Biochem. 195*, 203−213.

Tsuboi, M. (1962) *J. Polymer. Sci. 59*, 139−153.

Tytgat, J., & Hess, P. (1992) *Nature 359*, 420−423.

Wolfe, W. F., & Zissis, G. J. (1978) in *The Infrared Handbook*, U.S. Government Printing Office.

Wu, C. S. C., Ikeda, K., & Yang, J. T. (1981) *Biochemistry 20*, 566−570.

Yang, N., George, A. L., Jr., & Horn, R. (1996) *Neuron 16*, 113−122.

BI952988T